Parameter identification of continuum models for localized failure

C. Iacono & L. J. Sluys
Faculty of Civil Engineering & Geosciences, Delft University of Technology. Delft, The Netherlands.

ABSTRACT: The parameter identification problem of the gradient-enhanced continuum damage model is solved using tools of the inverse problems theory. Particularly, the K-Nearest Neighbors (KNN) technique and the Kalman Filter (KF) method are adopted in cascade to identify the length scale parameter and the parameter governing the softening branch of the material constitutive law. Two experimental data series are used, concerning different sizes and loading conditions, in order to investigate the influence of the involved experimental data in the parameter estimates and the predictive capabilities of the considered model. The inverse problem results to be ill-posed if only force-deformation data are used in the parameter identification procedure. Additional data related to the evolution of the width of the damaged zone during the fracture process are adopted in order to recover the well-posedness of the inverse problem.

1 INTRODUCTION

In the last three decades there has been an increasing interest in the study of the tensile behavior of concrete or, more generally, of quasi-brittle materials, in order to numerically simulate the strain localization process responsible for macroscopic fracture phenomena. However, the different computational models developed for this purpose contain some model parameters (constants) that cannot be directly measured during laboratory tests. For those model parameters the solution of an inverse problem is required, which can provide the parameter estimates by minimizing, iteratively, the discrepancy between experimental and computational data. This is the case, for instance, for the length scale parameter and the slope of the softening branch of the material constitutive law of the gradient-enhanced continuum damage model, on which the present paper focuses. Different issues of the parameter identification procedure are investigated, as for instance the well-posedness of the inverse problem and the predictive capabilities of the calibrated model in terms of size and geometry effects. For this purpose, the K-Nearest Neighbors (KNN) technique associated with the Kalman Filter (KF) method is adopted. Experimental data from uniaxial tensile tests and three point bending tests of different specimen sizes are used.

2 COMPUTATIONAL MODEL

The adopted computational model (for a complete treatment see Peerlings (1999)) is based on the isotropic continuum damage formulation of Lemaitre and Chaboche (1990), containing a damage scalar variable ω responsible for the degradation of the elastic properties of the material according to the following classical stress-strain relation

$$\boldsymbol{\sigma} = (1-\omega)\boldsymbol{D}^{el}\boldsymbol{\varepsilon} \tag{1}$$

in which $\boldsymbol{D}^{el}$ is the matrix of the undamaged ($\omega = 0$) elastic stiffness moduli. The damage process is driven by the modified von Mises definition of the equivalent strain ε_{eq} (Vree et al. 1995), that after reaching a certain strain threshold triggers the damage evolution according to an exponential softening damage evolution law. The model is regularized through the introduction of a nonlocal equivalent strain $\bar{\varepsilon}_{eq}(\boldsymbol{x})$ as an average quantity of the local counterpart $\varepsilon_{eq}(\boldsymbol{x})$ on a certain radius of the material point that is governed by a model parameter l, referred to as the length scale. Hence, the following diffusion equation (implicit gradient formulation) is added to the material constitutive laws

$$\bar{\varepsilon}_{eq} - c\nabla^2\bar{\varepsilon}_{eq} = \varepsilon_{eq} \tag{2}$$

where c is the so-called gradient parameter, which can be related to the length scale parameter ($c = l^2/2$). The described model contains seven model parameters to be identified (Iacono et al. 2006a): Young's modulus, Poisson's ratio, the tensile and compressive strengths of the material, the gradient parameter c and two parameters β and α governing, respectively, the

negative slope and the tail of the softening branch of the material constitutive law. For computing time reasons, the parameters identification procedure presented in this paper focuses on c and β, considering the remaining parameters as a priori known.

3 INVERSE PROBLEM

Solving the forward problem means to find analytical or numerical solutions for the ordinary or partial differential equations of the model, with known initial and boundary conditions and constants (or parameters) in the equations. On the contrary, in the inverse problem the solution is known and the objective is to determine the complete forward problem for which that solution is possible.

3.1 *Inverse problems in experimental-numerical research*

Once a numerical model can provide qualitatively acceptable output, in comparison with the real responses of the described system, a rigorous estimation of the model parameters is needed, in order to reproduce quantitatively correct output.

Let S be the real mechanical system represented by a numerical model containing model parameters assembled in a vector $\mathbf{x}$. If a perturbation is applied on S, the system reacts giving a certain response representable by a certain number of quantities measured at different 'instants' t and collected in a $\mathbf{y}^t_{\text{exp}}$ vector. On the other hand, the numerical model of the system, given the model parameter vector $\mathbf{x}$, is able to compute the solution of the forward problem $\mathbf{y}^t_{\text{comp}}$, as the corresponding computational counterpart of $\mathbf{y}^t_{\text{exp}}$. The correct estimate of the model parameters vector $\mathbf{x}$ may be obtained using inverse techniques, which, starting from an initial guess of the model parameters $\mathbf{x}_0$, minimize a function $f(\mathbf{x})$ (objective function) of the discrepancy between $\mathbf{y}^t_{\text{exp}}$ and $\mathbf{y}^t_{\text{comp}}$

$$f(\mathbf{x}) = (\mathbf{y}^t_{\text{exp}} - \mathbf{y}^t_{\text{comp}}(\mathbf{x}), \mathbf{x}_0) \tag{3}$$

This calibration phase of the model development represents a first check for the model. In fact, for instance, the solution of the inverse problem might not exist or it might be unstable. The identification of the sources of error may require a significant effort, since causes of ill-posedness might not only be found in the model, but also in the type of experimental data used for the calibration (quality, quantity and type of data) or in the adopted inverse method (for instance, local search techniques might stick into local minima of the objective function).

Hence, the inverse analysis might reveal limits in the basic assumptions of the model. A 'proof ab absurdo' of the model can be provided by the inverse analysis: starting from the hypothesis that the way the model describes the physical process is correct, possible flaws might be found, that lead to re-discuss the hypotheses, which give input for model improvements.

However, for a rigorous model assessment various real situations needed to be considered, *different* from the one(s) used for the model calibration. Forward problems are solved and comparisons between the experimental and computational responses are performed. Hence, limits related to the predictive capacities and to the applicability of the model can be provided, in order to have a model as a valid tool for design, monitoring, and prediction problems.

If, on one hand, experimental data may be used for qualitative and quantitative updating of the numerical model, on the other hand, the numerical model may be a useful tool for the optimal experiment design (several criteria and methods are available (Emery and Nenarokomov 1998)). For instance, numerical simulations may lead to optimal choices for measurement set-up, regarding, for instance, number of sensors, their location, geometry and size of the specimen, boundary and loading conditions, duration of the experiment, etc. Hence, the continuous integration and interaction of model building with experimental testing allows not only the complete understanding of a real phenomenon, but also significant improvement of both experiments and numerical modelling. Within this framework, the Inverse Problems Theory can provide the tools to connect experimental and computational research.

3.2 *Inverse techniques*

The choice of the inverse technique is fundamental. More inverse techniques may be used, for instance in cascade, in order to optimize *effectiveness* (how close the estimation is to the exact solution), *efficiency* (time saving) and *robustness* (reliability or repeatability of the solution) of the method.

In the present work, two inverse techniques, briefly described below, are used in cascade, with different features, so that a compromise of local-global search tool is obtained: the K-Nearest Neighbors (KNN) method and the Kalman filter (KF) method.

The basic notions of their mathematical formulation are presented in Iacono et al. (2003), (2006a), while detailed treatments can be found in e.g. Kailath et al. (2000), Tarantola (1987), Bittanti et al. (1984), Catlin (1989), Bui (1994), Powell (1998). Here, it suffices to mention that, since the final solution may be strongly influenced by the starting point of the search process, the KNN method is proposed for a first preliminary study of the parameters space. In this way, possible ill-posedness of the inverse problem may be easily detected and promising search regions may be localized, speeding up the convergence of the inverse

procedure and avoiding model parameter estimates representing local minima of the objective function. The KNN method is also suggested when a rough tuning of a model is required, because it may be easily handled (derivative free method) and implemented for any computational model (without changing the forward problem code, but as an external tool) and also by users that are not familiar with the inverse problem theory.

Successively, using the so-identified parameters vector as initial guess, the KF method is adopted in order to refine the inverse solution. The KF method takes into account also the uncertainties related to the experimental data and to the parameter estimates, offering also the advantage of a subsequent parameter update during the fracture process.

4 EXPERIMENTAL DATA

Two experimental data series, reported below, are used in the present paper.

4.1 *Series no. 1*

The series no. 1 is represented by tensile size effect tests on concrete dog-bone shaped specimens carried out in the Stevin laboratory of Delft University of Technology (van Vliet 2000), (van Vliet and van Mier 2000). The available experimental data are the *global* load-displacement curves for the various specimen sizes.

4.2 *Series no. 2*

This series consists of double-edge notched uniaxial tensile tests and single-edge notched bending tests on specimens made of the same concrete (Hariri 2000), (Hariri 2001). In this case, besides conventional measurement techniques such as using LVDTs, in-plane Electronic Speckle Pattern Interferometry (ESPI) is used leading to whole field displacements and strain distributions along the main sensitivity direction perpendicular to the notches. Hence, the available experimental data consist of global data (force vs. deformation curves) and *local* data (width of the fracture process zone vs. deformation curves) for the different specimen sizes and geometries (see Section 7). This data series allows a relevant investigation of four essential aspects: i) which kind of experimental data is necessary for the identifiability of the model parameters and the well-posedness of the inverse problem (local/global data), ii) how the estimated parameters are influenced by the experimental data involved in the inverse problem iii) the assessment of the reliability of the model predictions, in terms of loading conditions and size effects.

5 UNIQUENESS OF THE INVERSE SOLUTION

If only the force-deformation curve (global data) is considered and an approximation of the objective function of Eq. (3) is built, using the KNN method, a saddle shaped surface appears. This is shown in Figure 1a, for instance, in case of the dog-bone specimen type C of the experimental series no. 1. This means that the two model parameters β and c are correlated. The inverse problem is ill-posed, since no unique and/or stable solution is guaranteed. Hence, different parameter sets correspond to similar global force-deformation curves (Iacono et al. 2006a).

The well-posedness of the inverse problem is not recovered when the global data of different specimen sizes are considered, as shown in Figure 1b, being the coupling between the parameters c and β of a similar type for all sizes (Iacono et al. 2004), (Iacono et al. 2006a).

6 SIZE EFFECT

The gradient-enhanced damage model seems to incorrectly reproduce the entire experimental size effect curve, using only one parameters set for all specimen sizes: the computational size effect curve remains too flat compared to the experimental one (Iacono et al. 2006b). By using a single parameter set for all specimen sizes and involving only global data, only an *unstable average* fitting of the size effect curve can be reached. In other words, different parameter sets can be found which correspond to slightly different computational size effect curves, representing an average fitting of the experimental curve. This is shown in Figure 2a for the case of the bending tests of the experimental series no. 2 (where the considered parameter set belongs to the saddle of the objective function $f(\mathbf{x})$).

A better fit may be achieved considering a fixed value of $\beta = 500$ and different values of the gradient parameter c, as shown in Figures 2b and 3.

7 FPZ WIDTH

The width of the fracture process zone (FPZ), available in the experimental series no. 2, is used as additional information in order to solve the correlation between the two model parameters c and β.

However, the main difficulty is to establish a criterion in order to define the FPZ width d from a strain distribution. Experimentally, the use of in-plane Electronic Speckle Pattern Interferometry (ESPI) in the experimental series no. 2 provides whole field displacements and strain distributions along the main sensitivity direction perpendicular to the notches. Hence, the FPZ width is defined as the width of the area where the strain exceeds a certain threshold value, defined relatively to the peak value (in this case

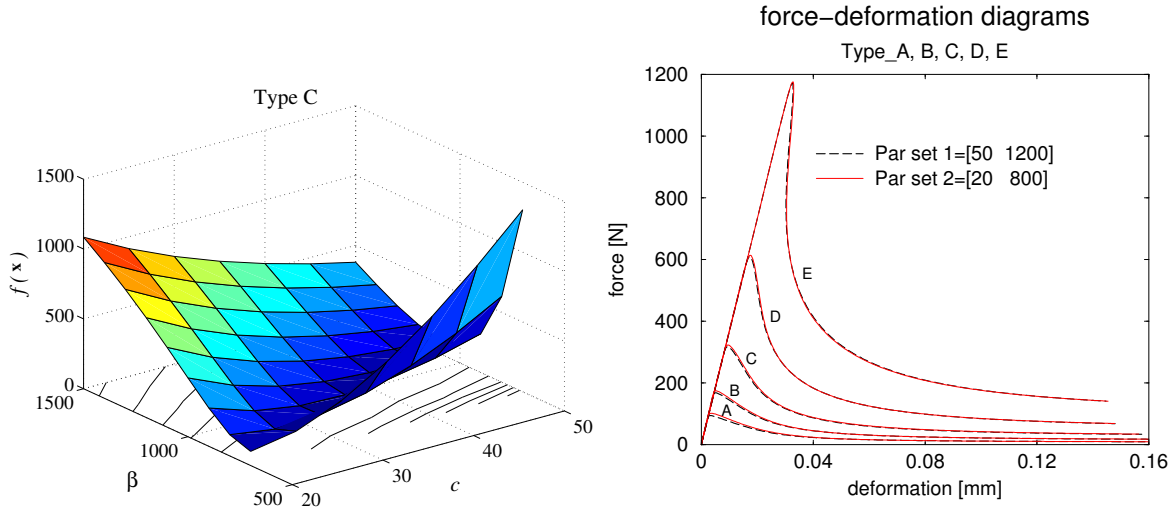

Figure 1. (a) Objective function $f_{\alpha=0.93}(\beta, c)$ for the type C dog-bone shaped specimen. (b) Force deformation curves for all dog-bone specimen sizes (A to E) for two equivalent parameter sets, set$_1$=$[c = 50\ \text{mm}^2\ \ \beta = 1200]$ and set$_2$=$[c = 20\ \text{mm}^2\ \ \beta = 800]$ ($\alpha = 0.93$).

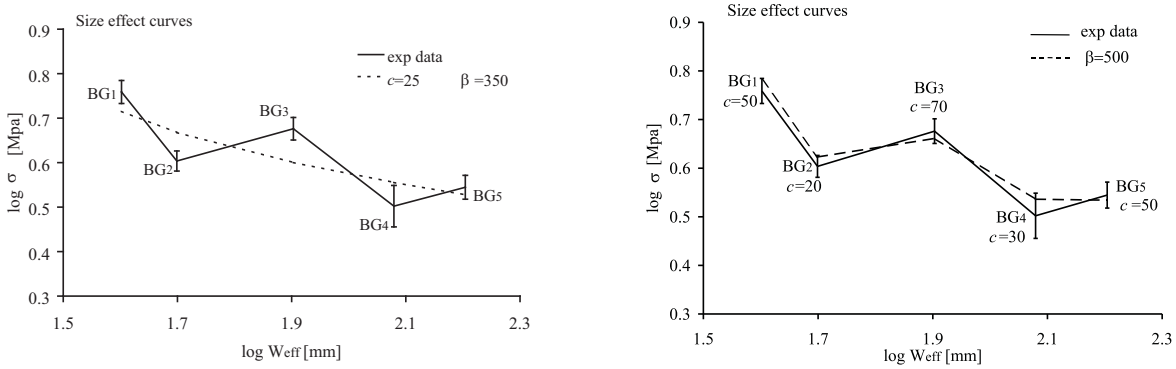

Figure 2. (a)Experimental and computational size effect curves for the single-edge notched bending specimens (BG1 to BG5 size) of the experimental series no. 2 (Hariri 2000), (Hariri 2001) ($\alpha = 0.92$) (b) corresponding computational size effect curve. The stress-CMOD curves related to these parameter sets are shown in Figure 3 ($\alpha = 0.92$).

20%). Widths of the FPZ are recorded during the entire fracture process, so that FPZ width vs. deformation curves are available for the experimental series no. 2.

Numerically, at each time step t, the nonlocal equivalent strain profile along the beam mid-height axis may be considered (alternatively, the damage profile or the local equivalent strain profile might be used). Hence, analogously to the experimental case, the computational value $d^t_{\text{comp}}(\mathbf{x})$ may be defined as the width of the area where the nonlocal strain $\bar{\varepsilon}_{eq}$ is larger than a certain fixed percentage (the same used during the experiments) of the peak value (see Figure 4).

It could be argued that this way of determining the FPZ width is arbitrary and debatable and that the final estimate of the model parameters vector is influenced by both the experimental technique adopted for the measurement of d_{exp} and the method and threshold value used for the definition of the numerical corresponding value d_{comp}. However, the essential aspect and requirement is that all coefficients, assumptions, and procedures used for the calibration of the numerical model are kept constant and consistent for all specimens sizes and loading conditions, so that the predictive capacity of the model may be assessed. Therefore, the strain threshold value used for the definition of the FPZ width, which should be consistent with the experimental data, may be seen as a tuning parameter of the so-calibrated model.

Hence, the width of the damaged area d may be included in the definition of the objective function $f(\mathbf{x})$ (Iacono et al. 2006a), according to

$$f(\mathbf{x}) = \sum_{j=1}^{n} p_1 f_{1\_sizej} + \sum_{j=1}^{n} p_2 f_{2\_sizej}, \qquad (4)$$

where f_{1_sizej} and f_{2_sizej} are the global and local contribution, respectively, related to the specimen size j. In Eq. (4), p_1 and p_2 are two weight factors with which the two contributions, global and local data, are taken into account (guidelines for the choice of their values are suggested in Iacono et al. (2006a)).

Hence, if only the global data or only the local data